



HAL
open science

Effect of temperature on the low cycle fatigue behavior of Glidcop Al-15

Abderrazak Daoud, Jean-Bernard Vogt, Eric Charkaluk, Lin Zhang,
Jean-Claude Biasci

► **To cite this version:**

Abderrazak Daoud, Jean-Bernard Vogt, Eric Charkaluk, Lin Zhang, Jean-Claude Biasci. Effect of temperature on the low cycle fatigue behavior of Glidcop Al-15. *Procedia Engineering*, 2010, 2, pp.1487-1495. 10.1016/j.proeng.2010.03.160 . hal-02512481

HAL Id: hal-02512481

<https://hal.univ-lille.fr/hal-02512481v1>

Submitted on 19 Mar 2020

HAL is a multi-disciplinary open access archive for the deposit and dissemination of scientific research documents, whether they are published or not. The documents may come from teaching and research institutions in France or abroad, or from public or private research centers.

L'archive ouverte pluridisciplinaire **HAL**, est destinée au dépôt et à la diffusion de documents scientifiques de niveau recherche, publiés ou non, émanant des établissements d'enseignement et de recherche français ou étrangers, des laboratoires publics ou privés.



Distributed under a Creative Commons Attribution - NonCommercial - NoDerivatives 4.0
International License



ELSEVIER

Available online at www.sciencedirect.com



Procedia Engineering 2 (2010) 1487–1495

Procedia
Engineering

www.elsevier.com/locate/procedia

Fatigue 2010

Effect of temperature on the low cycle fatigue behavior of Glidcop Al-15

Abderrazak Daoud^a, Jean-Bernard Vogt^{a*}, Eric Charkaluk^b, Lin Zhang^c, Jean-Claude Biasci^c

^aUniversité des Sciences et Technologies de Lille, Unité Matériaux et Transformations ENSCL/USTL, UMR CNRS 8207 Bâtiment C6 59655 Villeneuve d'Ascq Cedex France

^bEcole Centrale de Lille, Laboratoire de Mécanique de Lille, UMR CNRS 59655 Villeneuve d'Ascq Cedex France

^cEuropean Synchrotron Radiation Facility, 6 rue Jules Horowitz, BP220, 38043 Grenoble Cedex, France

Received 8 March 2010; revised 9 March 2010; accepted 15 March 2010

Abstract

Glidcop Al-15 is an Oxide Dispersion Strengthened (ODS) copper which has been widely used throughout the world in high-heat-loaded components because of its high strength especially at higher temperatures. At the European Synchrotron Research Facility (ESRF, Grenoble, France) the Glidcop Al-15 is used for manufacturing photon absorbers. It consists in two segments of OFHC (Oxygen-Free High Conductivity) copper brazed with another segment of Glidcop Al-15. This absorber is subjected to intense thermal stress cycles due to the high intensity X-ray beams.

This work aims at studying the fatigue behavior of the Glidcop Al-15 at high temperature (300°C). This study is divided into two parts: First the effect of heat treatment cycles which simulate brazing operation on Glidcop Al-15 will be analyzed. Then the effect of temperature on low cycle fatigue (LCF) behavior and failure mechanisms will be discussed.

© 2010 Published by Elsevier Ltd. Open access under [CC BY-NC-ND license](http://creativecommons.org/licenses/by-nc-nd/3.0/).

Keywords: Dispersion strengthened copper ; Glidcop ; Brazing ; Mechanical properties; Fatigue.

1. Introduction

The European Synchrotron Research Facility is operating with the third generation light sources in order to generate extremely powerful X-rays. Many critical components such as photon absorbers are used to control the exposure of downstream components to the intense X-rays. The crotch absorber, illustrated on Fig.1, is made of Glidcop Al-15, an Oxide Dispersion Strengthened (ODS) copper, and of Oxygen-Free High Conductivity (OFHC) copper. This component, located closest to the bending magnet, is the most critical one due to the high power density on it and the limited space for the installation. The front piece in 4 mm thick Glidcop is brazed with square

* Corresponding author. Tel.: +33 320 434 045; fax: +33 320 336 148.

E-mail address: jean-bernard.vogt@univ-lille1.fr.

copper tubes, 10 tubes per segment. The three segments of the sub-assembly are brazed with another 10 mm thick copper plate on the back [1]. The crotch absorber is subjected to intense thermal stress cycles from the high intensity X-ray beams. After several high heat load cycles under severe loading configuration, cracks can initiate and lead to the failure of this component [1-2].

Glidcop Al-15 has been widely used over the world in high-heat-load components owing to its high strength especially at higher temperatures [3]. Glidcop Al-15 is produced by the internal oxidation method [4-5]. The internal oxidation process provides a microstructure containing a very uniform distribution of fine aluminum oxide particles aimed at strengthening the ductile copper matrix. The degree of strengthening is a function of the size, shape, spacing, hardness, distribution, and coherency of the second-phase particle with the matrix [6-7]. Therefore, Glidcop Al-15 can serve as a potential high conductivity–high strength material since electrical and thermal conductivity of the matrix should not be strongly affected by the addition of a small amount of dispersoid particles incoherent with the metallic matrix. Indeed, Wycliffe founded that the only copper alloys with good strength above 650°C were ODS alloys such as Glidcop [8]. However, Wycliffe also noticed that the ductility and low cycle fatigue properties of ODS copper alloys were low at elevated temperatures.

This paper reports the preliminary results of a study aimed at predicting the thermal fatigue life of the Glidcop crotch absorbers. Here, the fatigue behavior of the Glidcop Al-15 is investigated at high temperature (300°C) taking into account the microstructure effect. Thus, the paper is composed of two parts. First the effect of heat treatment cycles which simulate brazing operation (HTSBO) on Glidcop Al-15 will be analyzed. Then the effect of temperature on LCF behavior and failure mode will be discussed.

2. Material and experimental procedures

The materials used in the present investigation is a low oxygen grade aluminum oxide (Al_2O_3) dispersion strengthened copper alloy (C15715), known and marketed by the trade name Glidcop Al-15. It contains 99.3% vol. (99.7 wt %) of copper and 0.70 vol % (0.3 wt %) of aluminum oxide [9, 10]. It is an extruded rod of 6.25 mm diameter. The material has been studied in the as received condition and after a heat treatment (HTSBO) simulating the brazing.

Tensile and fatigue tests have been performed on cylindrical specimens, taken from an extruded rod in the extrusion direction (10 mm diameter and a gauge length of 15 mm). A batch of specimens were subjected to the HTSBO treatment according to the cycle reported on Fig 2 while another one was machined just after reception.

Before testing, the specimens were mechanically polished on progressively finer grades of silicon carbide paper (220 to 4000) with water as lubricant, diamond paste ($3\mu\text{m}$ to $0.25\mu\text{m}$) with DP-lubricant red form Struers as lubricant and then electro-polished with Electrolyte D solution from Struers (voltage 24 volts) in order to avoid any premature crack initiation. For metallographic investigation, these steps were followed by chemical etching in 25 mL NH_4OH (28%) + 5 mL H_2O_2 (30%).

Tensile and fatigue tests were carried out on a servo-hydraulic machine. Tensile tests were carried out either at room temperature and at a constant strain rate of $2 \cdot 10^{-3} \text{ s}^{-1}$ or at $T=175^\circ\text{C}$ and a constant strain rate of $6.6 \cdot 10^{-3} \text{ s}^{-1}$. Low cycle fatigue (LCF) tests were performed under axial total strain control. A fully push pull mode ($R_e = -1$), a triangular waveform, different constant strain rate of 10^{-4} s^{-1} , $4 \cdot 10^{-3} \text{ s}^{-1}$ and total strain variation ranging from $\Delta\epsilon_t = 1.4\%$ to 0.6% were applied at room temperature and at 300°C .

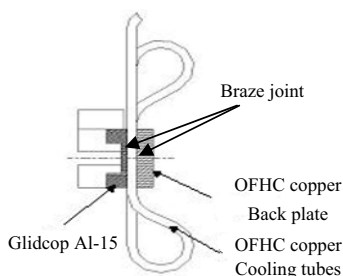


Fig 1: Different components of Crotch absorber

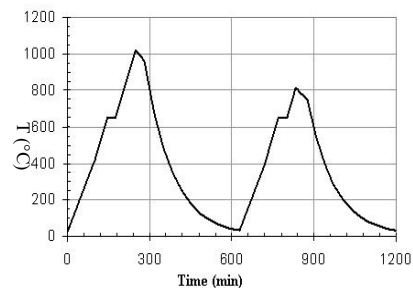


Fig 2: Brazing heat treatment cycle

The temperature is monitored and measured by a thermocouple in the gauge length of the specimen. The fatigue life N_f is defined as the number of cycles needed for a 25% drop in the tensile stress taking as a reference the stabilized hysteresis loop.

3. Results and analysis

3.1. Metallographic characterization and microstructure

At first, optical microscopy was employed for microstructure characterization but it appeared unsuccessful tool, due to the very small grain size of the material in the as received condition as well as in the heat treated one. Therefore, the microstructure was examined by SEM in the BSE mode on longitudinal and transverse section of the specimen. As can be seen in Fig.3, no major effect caused by the HTSBO is observed. Both materials have the same grain size of 0.2 μm in the transverse direction.

Additional investigation was performed by TEM on thin foil taken in the longitudinal and transverse orientations (Fig. 4).

The grain size of Glidcop Al-15 as-received condition is confirmed to range between 5 to 15 μm in longitudinal direction and 0.2 to 0.5 μm in transverse direction (see Fig. 4a).

The Al_2O_3 particles were uniformly dispersed in the copper matrix (Fig. 4b). These particles have a strong effect on the mobility of dislocations since they behave as strong obstacle to dislocation motion (Fig. 4c). This is the reason why Glidcop Al-15 has significantly higher yield stress and ultimate tensile strength in comparison to OFHC (Oxygen-Free High Conductivity) copper.

Though no statistical analysis on particle size has been made in the present work, they usually are in range from 3 to 12 nm with an inter-particle spacing of 30-100 nm and a particle density of 10^{16} to 10^{17} cm^{-3} [4]. The fine particles are hard and thermally stable even at temperatures approaching the melting point of the copper matrix. They do not coarsen but become less effective as barriers to the motion of dislocations [10].

The fine dispersion of the aluminum oxide particles in the copper matrix also moderates or prevents recrystallization and this effect depends on particles of appropriate size and distribution [11]. This agrees with our observations. In addition, it is suspected that the microhardness of Glidcop Al-15 should not show any change after heat treatment, what confirm its good solderability [7].

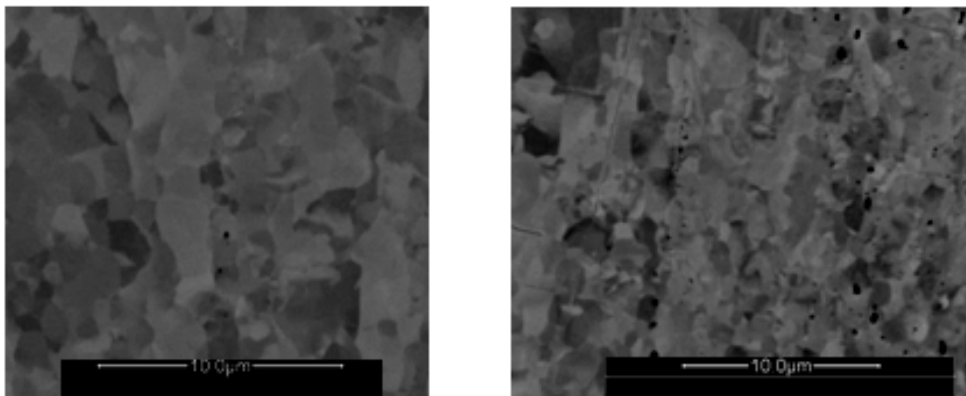


Fig. 3 : SEM –BSE micrographs showing the microstructure of Glidcop Al-15 in the transverse direction of the bar: (left) the as-received condition (right) after HTSBO

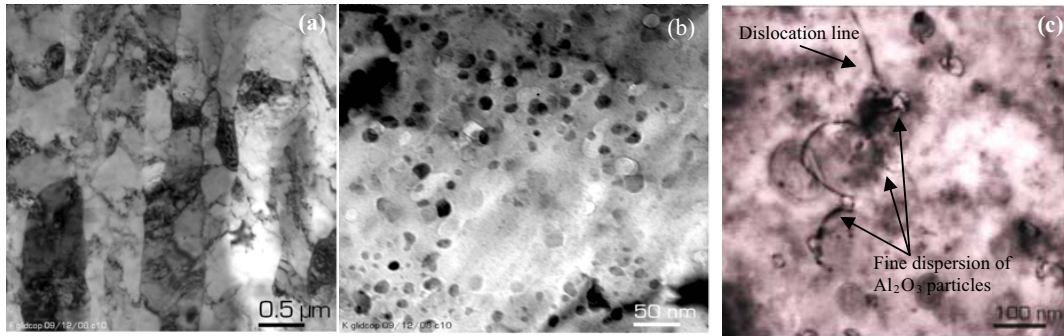


Fig 4: TEM micrographs showing: (a) grain size; (b) fine dispersion of Al₂O₃ in the copper matrix; (c) bowing of dislocations blocked by Al₂O₃ particles

3.2. Monotonic tensile behavior

3.2.1. Mechanical behavior

The stress-strain curve and the strain hardening characteristics of Glidcop Al-15 before and after HTBSO at room temperature and at 175°C are shown Fig.5a and 5b. The strain hardening characteristics are evaluated by examining the variation of true stress with true plastic strain plotted on a bilogarithmic scale. The variation of stress (σ_{tp}) with true plastic strain (ϵ_{tp}) follows power law:

$$\sigma_{tp} = k (\epsilon_{tp})^n \tag{1}$$

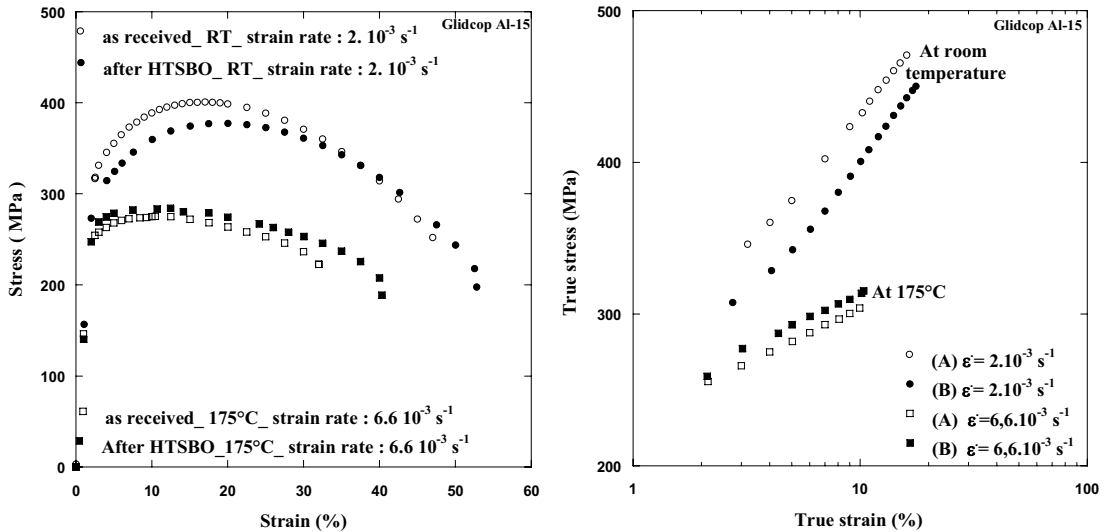


Fig. 5: Engineering stress-strain diagram (left) and variation of true stress versus true plastic strain of Glidcop Al-15 deformed at room temperature and at 175°C according to the heat treatment#

Table 1 collects the tensile properties of Glidcop Al-15 before and after HTSBO at room temperature and at 175°C.

Table1: Mechanical properties of Glidcop Al-15 obtained from monotonic tensile tests

Condition	$\dot{\epsilon}$ (s ⁻¹)	T (°C)	σ_y (MPa)	UTS (MPa)	A (%)	Au (%)	n	K (MPa)
As received	2×10^{-3}	25	325	401	47	14	0.19	275
After HTSBO	2×10^{-3}	25	300	377	52	17	0.21	242
As received	6.6×10^{-3}	175	245	275	32	11	0.11	235
After HTSBO	6.6×10^{-3}	175	253	284	40	8	0.10	246

At room temperature and at a strain rate of 2.10^{-3} s^{-1} , the HTSBO results in a small decrease of the yield stress and of the ultimate tensile strength. The yield stress decreased from 325 MPa to 300 MPa and the ultimate tensile strength decreased from 401 MPa to 375 MPa (diminution of 7.7% and 5.8% respectively), but the ductility is improved.

At 175°C and at a strain rate of $6.6.10^{-3} \text{ s}^{-1}$, the very small variations in the mechanical values, in the range of data scattering, does not allow to assign any effect of HTSBO. The HTSBO does not affect the mechanical properties.

Stephens et al showed that heat treatment cycles which simulate brazing operations as high as 980°C result in only a small decrease in ultimate tensile strength (13%) in Glidcop Al-15, and that ductility improves substantially [12]. The same conclusions are found by Henry et al when they study the effect of heat treatment to simulate a brazing operation as high as 935°C [13]. The same conclusions are made for the monotonic strain hardening exponent n and the monotonic strength coefficient k . At room temperature and with a strain rate of 2.10^{-3} s^{-1} , the HTSBO results in a small decrease of the monotonic strength coefficient k and a small increase of the monotonic strain hardening exponent n . The opposite is observed at 175°C and with a strain rate of $6.6.10^{-3} \text{ s}^{-1}$. A temperature effect is visible when tests at room temperature and at 175°C are compared. Indeed, the tensile properties decrease with increasing test temperature. Srivatsana et al explain this temperature effect by a partial relief of the compressive residual stresses induced by the manufacturing process and a local softening of the soft and plastically deforming copper matrix [10].

Stephens et al show that fine-grained Glidcop Al-15, annealed for 15 min at 980°C is stronger at room temperature than coarse-grained Glidcop Al-15 annealed 100 h at 980°C. But, as the test temperature increases, the advantage fine-grained Glidcop Al-15 vanishes, until at 800°C coarse grained Glidcop Al-15 is stronger than fine-grained Glidcop Al-15[14-15].

3.2.2. Fracture surface

Fig 7 corresponds to the SEM micrographs of the tensile fracture surfaces. At room temperature, there is no obvious difference on fracture morphology for Glidcop Al-15 before (A1) and after HTSBO (B1). The macroscopic aspect of the fracture surface is characterized by a helical shape, probably induced by the manufacturing process (extrusion). Other tests will be carried out to explain this shape.

All over the fracture surface, a uniform distribution of variable size and depth of voids are imaged at higher magnifications (A2), (B2). The formation and coalescence of microvoids confirms the ductility of Glidcop Al-15 at room temperature. There is no important difference between (A2), (B2) except the voids are deeper for Glidcop Al-15 in the as-received condition, hence increased ductility after HTSBO. At 175°C, the voids are smaller and less deep than at room temperature. At this temperature, the Glidcop Al-15 has the same fracture surface before and after HTSBO. Li et al found that the fracture surface morphology revealed for the Glidcop Al-25 alloys display ductile fracture by microvoids coalescence in the temperature range 20 to 300°C [16].

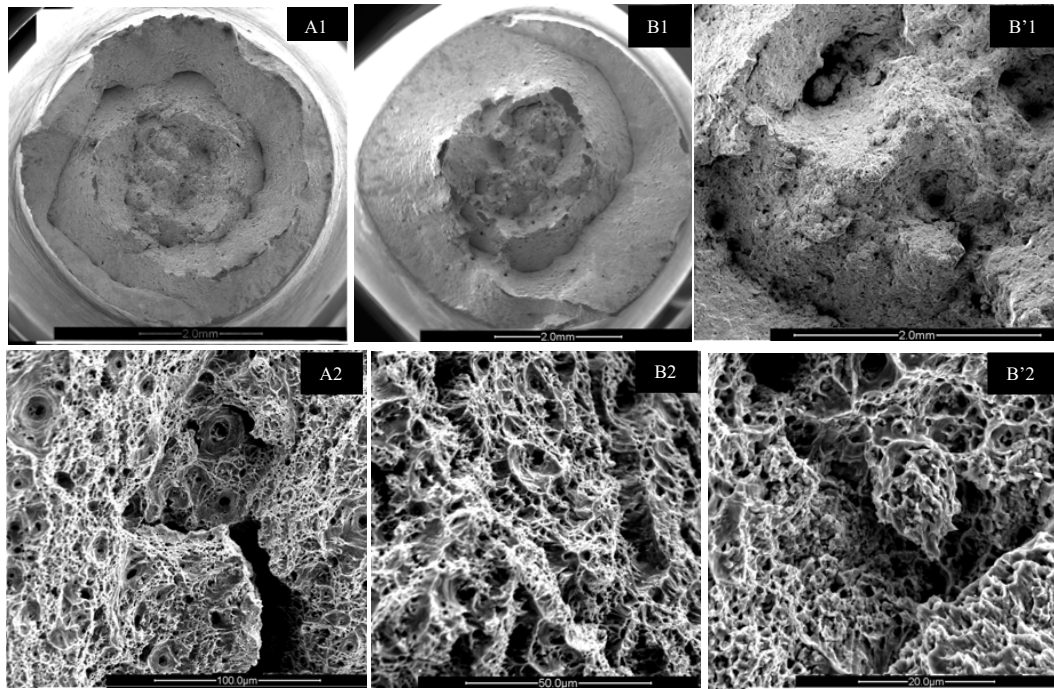


Fig9: SEM of the tensile fracture surfaces of the Glidcop Al-15: (A) as-received at room temperature; (B) after HTSBO at room temperature; (B') after HTSBO at 175°C.

3.3. Low Cycle Fatigue

3.3.1. Effect of HTSBO on LCF behavior of Glidcop Al-15

The evolution of the stress amplitude versus the number of cycles N in logarithmic scale is reported on fig 10 for tests carried out at room temperature and a strain rate of 10^{-4} s^{-1} . The Glidcop Al-15 at high total strain range presents slight hardening at the beginning of the fatigue test and stabilizes after 10 cycles, until the decrease of the stress amplitude which is related to the propagation of a macroscopic crack into the bulk conducting to the failure.

From table 2 which gathers the results obtained from fatigue test at room temperature, constant strain rate $4 \cdot 10^{-4} \text{ s}^{-1}$ and total strain range $\Delta\varepsilon_t = 1.2\%$ and 1.4% , there is no difference between the fatigue behavior of Glidcop Al-15 before and after HTSBO. They have the same fatigue life (the difference is less than 2%) and the same mechanical properties.

Table 2: Low cycle fatigue data of Glidcop Al-15: (A) the as-received condition; (B) after HTSBO

Condition	ε (s^{-1})	E (GPa)	σ_Y (MPa)	σ_a	$\Delta\varepsilon_t$ (%)	$\Delta\varepsilon_p$ (%)	$\Delta\varepsilon_c$ (%)	Number of failure N_{25}
(A)	10^{-4}	105	300	326	1.2	0.64	0.56	1000
(B)	10^{-4}	105	302	314	1.2	0.6	0.6	1200
(A)	10^{-4}	98	290	324	1.4	0.76	0.44	1000
(B)	10^{-4}	102	285	314	1.4	0.8	0.6	600

The hysteresis loop at mid-life ($N_f/2$) is taken as the reference value representing the behavior of the material.

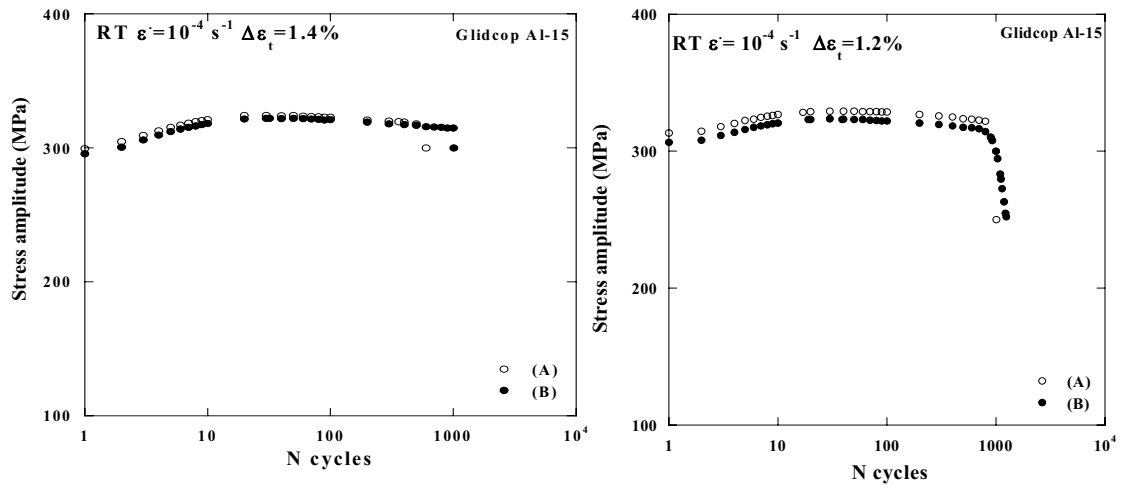


Fig10: Cyclic stress response for various strain range at room temperature of Glidcop Al-15: (A) the as-received condition; (B) after HTSBO

3.3.2 LCF at RT and 300°C of Glidcop Al-15 as-received

Stress evolution of tests carried out at room temperature and 300°C, at a strain rate of $4 \cdot 10^{-3} \text{ s}^{-1}$ are reported as a function of the number of cycles in a logarithmic scale (Fig. 11 a) and as a function of the life fraction in a linear scale (Fig. 11b).

For both test temperatures, at total strain range (1%- 6%), a slight hardening occurs at the very beginning of fatigue life (less than 2% of the total fatigue life). The stress amplitude stabilizes after 10 cycles during the main part of fatigue life. Then the propagation of macroscopic cracks leads to a characteristic decrease of the stress amplitude during less than 10% of fatigue life.

The stress amplitudes decrease when the temperature increases. Table 3 summarizes the fatigue properties of Glidcop Al-15 as received at RT and at 300°C.

Table 3: Fatigue properties of Glidcop Al-15 as received at 300°C

$\dot{\epsilon}$ (s^{-1})	T (°C)	σ_a	$\Delta\epsilon_t$ (%)	$\Delta\epsilon_p$ (%)	$\Delta\epsilon_c$ (%)	Number of cycles to failure
$4 \cdot 10^{-3}$	RT	325	1	0.4	0.6	1600
$4 \cdot 10^{-3}$	300	275	1	0.44	0.56	1500
$4 \cdot 10^{-3}$	RT	272	0.6	0.09	0.51	21300
$4 \cdot 10^{-3}$	300	218	0.6	0.1	0.5	12000

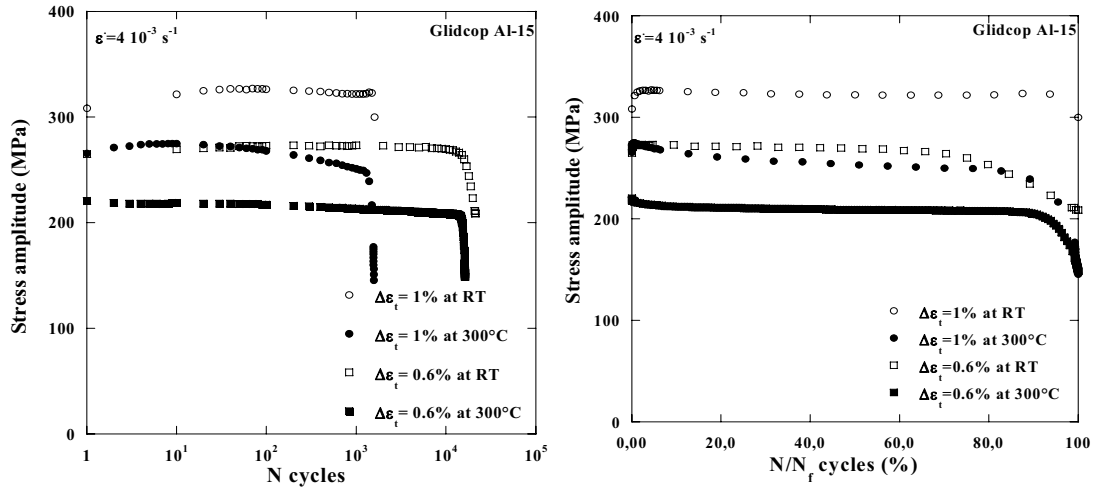


Fig11: Cyclic stress response as a function of the number of cycle: (a) and the life fraction (b) for various total strain range of ($\Delta\epsilon_t = 1\%$, $\Delta\epsilon_t = 0.6\%$) at RT and 300°C of Glidcop Al-15 as-received

The scanning electron micrograph examination of the sample gauge surface showed that the principal cracks growth path has an abrupt change of direction Fig.12a. Little or no secondary cracks are observed on the longitudinal cuts of sample. The morphologies of fracture surface are rather tortuous with a fracture surface at about 30° to 45° with respect to the loading axis Fig.12 b. Multiple initiation sites from which cracks have propagated into the bulk are observed.

This tortuous morphology and the multiple initiation sites reveal that the macroscopic crack occurs by joining some fatigue fracture surfaces initiated at different height in the gauge length. We observed easily the fatigue striations with a large spacing between them which induces that the propagation part is very rapid (during less than 10% of fatigue life).

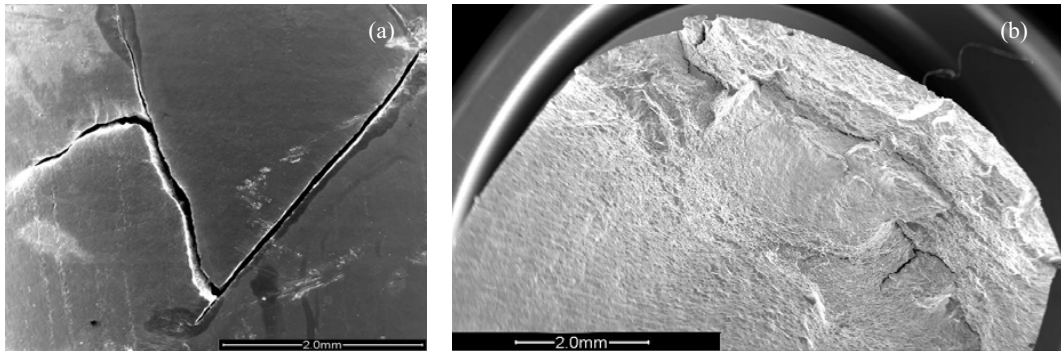


Fig12: The scanning electron micrograph of (a) the sample gauge surface; (b) the fracture surface.

4. Conclusions

In the present work based on investigations on an oxide dispersion strengthened copper alloy, the following observations are made:

- The influence of heat treatment reproducing the brazing operation is negligible and insignificant on Glidcop Al-15 in terms of: metallographic and microstructure, tensile and cyclic stress response at high strain range in low cycle fatigue.
- The tensile fracture morphology features reminiscent of ductile failure (formation and coalescence of microcavities and voids)
- The low cycle fatigue behavior of Glidcop Al-15 presents slight hardening at the beginning and stabilizes after 10 cycles, until the decrease of the stress amplitude is related to the propagation of a macroscopic crack during less than 10% of fatigue life.

References

- [1] Zhang L, Biasci J-C, Plan B. ESRF Thermal Absorbers Temperature Stress and Material Criteria. *2nd International Workshop on Mechanical Engineering Design of Synchrotron Radiation Equipment and Instrumentation* ; September 5-6, 2002 – Advanced Photon Source, Argonne National Laboratory, Argonne, Illinois U.S.A.
- [2] Ravindranath V, Sharma S, Rusthoven B, Gosz M, Zhang L, Biasci J-C. Thermal Fatigue Life Prediction of Glidcop® Al-15.
- [3] Sunao T, Mutsumi S, Mochizuki T, Watanabe A, Kitamura H. Fatigue life prediction for high-heat-load components made of Glidcop by elastic-plastic analysis; *J. Synchrotron Rad.* (2008). **15**, 144–150
- [4] Nadkarni AV, Troxell JD, Verniers F. GlidCop: dispersion strengthened copper: an advanced copper alloy system for automotive and aerospace applications; Internal Report; SCM Metal Products Inc; Cleveland, OH, USA.
- [5] Afshara A, Simchi A. Abnormal grain growth in alumina dispersion-strengthened copper produced by an internal oxidation process; *Scripta Materialia*; **58** (2008) 966–969.
- [6] Groza JR, Gibeling JC. *Mater Sci Eng Part A*; 1993; **A 171**: 115-125.
- [7] Troxell J-D. Glidcop dispersion strengthened copper: potential applications in fusion power generators; SCM Metal Products Inc.
- [8] Wycliffe P. Literature Search on High Conductivity Copper Based Alloys. Final Report IDWA No. 6458-2, Rockwell International Sci. Center, R5739TC/sn, 1984.
- [9] Arzt E, Rosler J. *Acta Metall*; 1988; **36**:1053
- [10] Srivatsana T, Narendrab N, Troxell J-D. Tensile deformation and fracture behavior of an oxide dispersion strengthened copper alloy; *Materials and Design* **21** -2000. 191- 198.
- [11] BARBERY J. Traitements thermiques du cuivre et de ses alliages. *Techniques de l'Ingénieur, traité Matériaux métalliques* ; M- 1295
- [12] Stephens J J and Schmale T-D. The Effect of High Temperature Braze Thermal Cycles on Mechanical Properties of a Dispersion Strengthened Copper Alloy; SANDIA REPORT 1987.
- [13] Henry C. deGroh II, David L E, William S. Loewenthal. Comparison of GRCop-84 to Other Cu Alloys with High Thermal Conductivities. *Journal of Materials Engineering and Performance*: 594 Volumes 17; 2008.
- [14] Stephens J J, Bourcier R J, Vigil F J, Schmale D T. Mechanical Properties of Dispersion Strengthened Copper : A Comparison of Braze Cycle Annealed and Coarse Grain Microstructure; Sandia Report SAND88-1351, 1988.
- [15] Rigollet, C. Contribution to the study of high temperature deformation and damaging mechanisms in an alumina strengthened copper. 1995.
- [16] Li M, Heuer J-k, Stubbins J-F, Edwards D-J. Fracture behavior of high-strength, high-conductivity copper Alloys. *Journal of Nuclear Materials*; **283-287** (2000) ;977-981.